Journal of Sustainable Bioenergy Systems, 2020, 10, 52-61
https://www.scirp.org/journal/jsbs
ISSN Online: 2165-4018
ISSN Print: 2165-400X

One-Dimensional Study of Thermal Behavior of Typha Panel: Spectroscopy Characterization of Heat Exchange Coefficient on Front Face

Sokhna Khadidiatou Ben Thiam[1], Alassane Ba[1], Mamadou Babacar Ndiaye[2], Issa Diagne[3], Youssou Traore[3], Seydou Faye[3], Cheikh Thiam[1], Pape Touty Traore[3], Ablaye Fame[1], Gregoire Sissoko[3]

[1]Ecole Polytechnique de Thiès (EPT), Thiès, Senegal
[2]University Institute of Technology, University of Thiès, Thiès, Senegal
[3]Laboratory of Semiconductors and Solar Energy, Physics Department, Faculty of Science and Technology, University Cheikh Anta Diop, Dakar, Senegal
Email: gsissoko@yahoo.com

How to cite this paper: Thiam, S.K.B., Ba, A., Ndiaye, M.B., Diagne, I., Traore, Y., Faye, S., Thiam, C., Traore, P.T., Fame, A. and Sissoko, G. (2020) One-Dimensional Study of Thermal Behavior of Typha Panel: Spectroscopy Characterization of Heat Exchange Coefficient on Front Face. *Journal of Sustainable Bioenergy Systems*, **10**, 52-61.
https://doi.org/10.4236/jsbs.2020.102005

Received: April 9, 2020
Accepted: May 22, 2020
Published: May 25, 2020

Abstract

Convective heat transfer coefficients, materializing exchanges between solid wall (here typha) and its environment, influence its behavior under excitation pulse. Temperature of wall and its density of flow vary with these coefficients according to its thickness (in depth). This study therefore focuses on the evaluation of convective heat transfer coefficient on front face and the optimal insulation thickness.

Keywords

Typha, Heat Transfer Coefficients, Spectroscopy, Optimal Insulation Thickness

1. Introduction

Use of local insulation materials from vegetable (biodegradable) or mineral origin [1] is alternative for environmental protection, on the one hand, and needs to ensure good energy efficiency [2] [3], on the other hand. Use of synthetic materials (polystyrene [4] [5], polyurethane [6] [7], glass wool [8] [9]) guarantees efficiency and profitability, but is nevertheless harmful to environment [10]. Option of substituting and/or combining synthetic materials with natural ones (local materials) has been subject of several research studies [11]-[16]. To ensure good insulation of buildings, material must have low thermal conductivity and be able to stand heat exchanges between it and its surrounding environment.

External parameters that can influence behavior of wall are: excitation pulse, solar radiation and convection coefficients [17]. Knowledge of thickness of insulation material is also an important parameter to consider for optimal insulation [18] [19] [20].

Heat transfer coefficient influences behavior of the material in response to excitations it undergoes. It materializes heat exchanges between walls of material and its surrounding environment (exterior and interior). Much research has focused on his determination [21]-[26].

In this paper, we will study spectroscopy of convection coefficient at front face of typha panel [27] [28] and also determine corresponding optimal thickness of insulator.

2. Theory

2.1. Study Model

Study model is shown in **Figure 1**, it is panel made of typha with thickness L. Transverse dimensions are large enough to consider that heat transfer is unidirectional. Heat exchanges between material and two sides (exterior and interior) are assumed to be convective. They are quantified by heat transfer coefficients on front and back sides.

- T_1 (˚C) and T_2 (˚C): temperature in frequency dynamic mode of external and indoor environment respectively;
- T_{01} and T_{02} (˚C): maximum amplitude of T_1 and T_2 respectively;
- T_0 (˚C): initial temperature of insulating material;
- L (m): length of material along x-axis;
- h_1 and h_2 ($W \cdot m^{-2} \cdot K^{-1}$): heat transfer coefficient at front and back face panel respectively.

2.2. Mathematical Formulation

Conservation of energy at any point of material is governed by following heat equation:

$$\rho C \frac{\partial T}{\partial t} = \frac{\partial}{\partial x}\left(\lambda \cdot \frac{\partial T}{\partial x} \right) + P \quad (1)$$

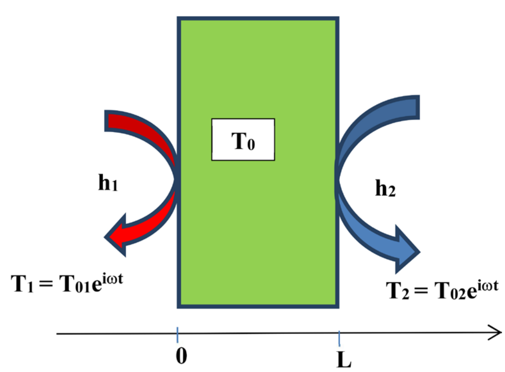

Figure 1. Wall typha.

where:

- ρ (kg·m^{-3}): density of material;
- C (J·kg^{-1}·K^{-1}): mass thermal capacity;
- λ (W·m^{-1}·K^{-1}): thermal conductivity of material;
- P (W·m^{-3}): internal heat supply (heat sink) of material;
- x (m): depth position.

Simplified form of this equation, in absence of internal heat sinks and for constant thermal conductivity (assumed isotropic material) is given by:

$$\frac{\partial T}{\partial t} = \frac{\lambda}{\rho Cp} \cdot \Delta T \tag{2}$$

Study is done in one dimension and equation becomes:

$$\frac{\partial^2 T\left(x,h_1,h_2,\omega,t\right)}{\partial x^2} = \frac{1}{\alpha}\frac{\partial T\left(x,h_1,h_2,\omega,t\right)}{\partial t} \tag{3}$$

where:

- $T\left(x,h_1,h_2,\omega,t\right)$: Temperature in material.

$$\alpha = \frac{\lambda}{\rho Cp} \tag{4}$$

- h_1: heat exchange coefficient front face;
- h_2: heat exchange coefficient rear face;
- α: Thermal diffusivity coefficient of the material (m^2·s^{-1}).

Solving this equation requires establishment of boundary conditions:

$$\lambda \left.\frac{\partial T}{\partial x}\right|_{x=0} = h_1\left(T\left(0,h_1,h_2,\omega,t\right) - T_1\right) \tag{5}$$

$$-\lambda \left.\frac{\partial T}{\partial x}\right|_{x=L} = h_2\left(T\left(L,h_1,h_2,\omega,t\right) - T_2\right) \tag{6}$$

Form of the solution of Equation (3) in dynamic frequency regime is:

$$T\left(x,h_1,h_2,\omega,t\right) = A\sinh\left(\beta x\right) + B\cosh\left(\beta x\right)\mathrm{e}^{i\omega t} + T_0 \tag{7}$$

where:

$$\beta = \sqrt{\frac{\omega}{2\alpha}}\left(1+i\right) \tag{8}$$

$\frac{1}{\beta}$: complex diffusion length.

Expression of heat flow density

$$\boldsymbol{\varphi} = -\lambda\, \boldsymbol{grad} T \tag{9}$$

φ (W·m^{-2}): heat density flow modulus, After resolution of Equation (9), we obtain the following expression:

$$\varphi\left(x,h_1,h_2,\omega,t\right) = -\lambda\beta A\cosh\left(\beta x\right) + B\sinh\left(\beta x\right)\mathrm{e}^{i\omega t}. \tag{10}$$

2.3. Spectroscopic Expression of Heat Exchange Coefficient

To determine spectroscopic expression of heat exchange coefficient h_1 at front face, we first study evolution of heat density flow as function of heat exchange coefficient at rear face h_2 (**Figure 2**).

Heat density flow increases with h_2 and reaches maximum for $h_2 > 50$ $W \cdot m^{-2} \cdot K^{-1}$; derivative function of heat density flow (11) allows to obtain the expression of h_1 (13).

$$\frac{\partial \varphi(x,h_1,h_2,\omega,t)}{\partial h_2} = 0 \quad (11)$$

$$\frac{\partial \varphi(x,h_1,h_2,\omega,t)}{\partial h_2} = -\lambda\beta\left[\frac{\partial A \cosh(\beta x)}{\partial h_2} + \frac{\partial B \sinh(\beta x)}{\partial h_2}\right] e^{i\omega t} = 0 \quad (12)$$

Resolution of Equation (12) allows us to obtain following expression:

$$h_1(L,\omega,t) = -\frac{(\lambda\beta)^2 \sinh(\beta L)\left(T_{02} - T_0 e^{-i\omega t}\right)}{(\lambda\beta)\cosh(\beta L)\left(T_{02} - T_0 e^{-i\omega t}\right) + \left(T_0 e^{-i\omega t} - T_{01}\right)}. \quad (13)$$

3. Results and Discussions

Figure 3 shows evolution of heat exchange coefficient h_1 as function of excitation pulse under thickness influence. Heat transfer coefficient increases with excitation for the different thickness values. Each maximum of h_1 corresponds to resonance frequency ω_r.

Cutoff frequencies ω_c are intersections of tangent lines of two consecutive parts of the concavity of curve.

Table 1 shows that resonant and cutoff frequencies increase as depth decreases. Maximum value of heat exchange coefficient for a resonant frequency decreases with thickness of insulating panel.

Figure 4 gives us the variation of h_1 as a function of thickness, taking into account the resonance frequencies. The heat transfer coefficient increases with the

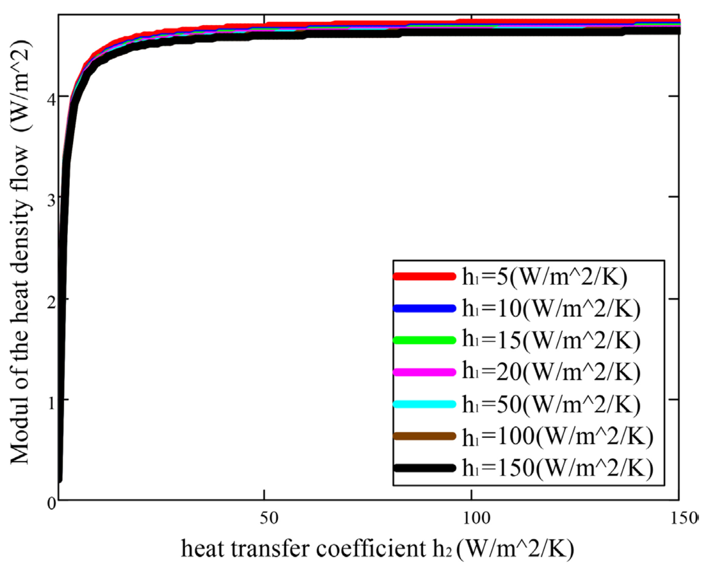

Figure 2. Module of heat flux density versus heat transfer coefficient at the rear face: influence of h_1, $\omega = 10^{-3.7}$ $rad \cdot s^{-1}$.

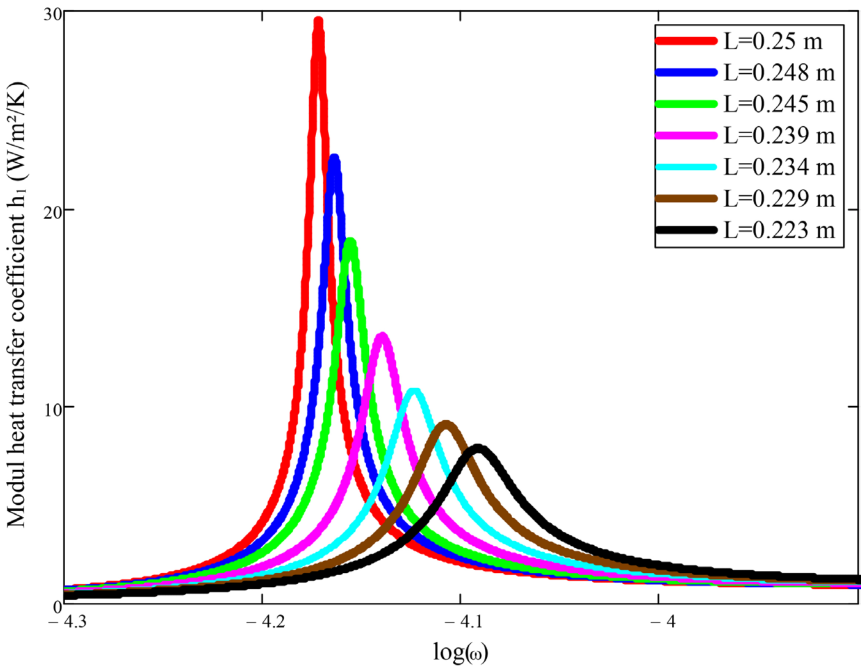

Figure 3. Evolution of h_1 as function excitation pulse ω (rad.s^{-1}); influence of thickness.

Table 1. Determination of resonance and cut-off frequency.

thickness (m)	0.25	0.248	0.245	0.239	0.233	0.229	0.223
h_{1max} (W·m^{-2}·K^{-1})	29.5	22.58	18.38	13.52	10.79	9.07	7.86
ω_c (rad/s)	$10^{-4.207}$	$10^{-4.201}$	$10^{-4.188}$	$10^{-4.184}$	$10^{-4.167}$	$10^{-4.166}$	$10^{-4.144}$
	$10^{-4.133}$	$10^{-4.124}$	$10^{-4.121}$	$10^{-4.095}$	$10^{-4.066}$	$10^{-4.052}$	$10^{-4.032}$
ω_r (rad/s)	$10^{-4.171}$	$10^{-4.164}$	$10^{-4.156}$	$10^{-4.139}$	$10^{-4.123}$	$10^{-4.107}$	$10^{-4.09}$

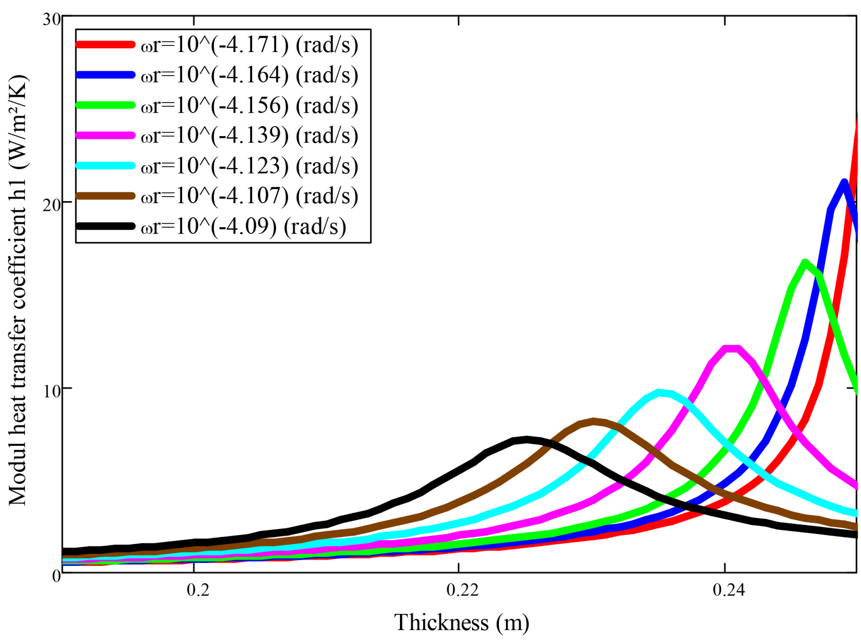

Figure 4. Evolution of h_1 as function of thickness; influence of resonance pulse ω_r.

thickness of the material and reaches a maximum value. This maximum of h_1 corresponds to a minimum thickness that allows good insulation.

In fact, higher heat transfer coefficient on front panel, thicker insulating panel. This thickness is called optimal thermal insulation thickness: X_{op} (Table 2).

Maximum of heat transfer coefficient is more important when pulsation is low, this corresponds to an increase of heat flow in material due to excitation. Indeed, period being inversely proportional to excitation frequency, latter lasts longer optimal insulation thickness decreases due to relaxation phenomena.

When material thickness exceeds optimal thickness, heat transfer coefficient on front face of panel decreases, which means that heat transfer coefficient no longer, has any influence on material's behavior.

Figure 5 is obtained from Table 2, in fact, we were able to plot logarithm of maximum heat transfer coefficient $h_{1\max}$ as function of logarithm of optimal thickness X_{op}.

The resulting curve can be assimilated linear function characterize by equation:

$$\log\left(h_{1\max}\right) = a\log\left(X_{op}\right) + b \tag{14}$$

$$h_{1\max} = \mathrm{e}^{b}\left[X_{op}\right]^{a} \tag{15}$$

Coefficients a and b are determined from curve by using Equation (15).

$$h_{1\max} = 1.48 \times 10^{8}\left[X_{op}\right]^{11.32} \tag{16}$$

Figure 6 and Figure 7 show respectively phase diagram of the heat transfer coefficient and its corresponding Nyquist representations for different values of the material thickness [29].

Table 2. Resonance pulse and optimal depth value for $h_{1\max}$.

h_{1max} ($W \cdot m^{-2} \cdot K^{-1}$)	23.39	21.051	16.734	12.057	9.693	8.144	7.125
ω_r ($rad \cdot s^{-1}$)	$10^{-4.171}$	$10^{-4.164}$	$10^{-4.156}$	$10^{-4.139}$	$10^{-4.123}$	$10^{-4.107}$	$10^{-4.09}$
X_{op} (m)	0.25	0.249	0.246	0.241	0.236	0.23	0.225

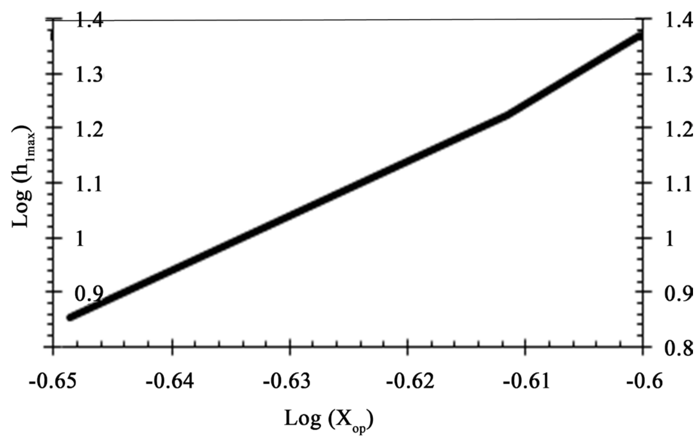

Figure 5. Maximum values of h_1 as function of optimal thickness values.

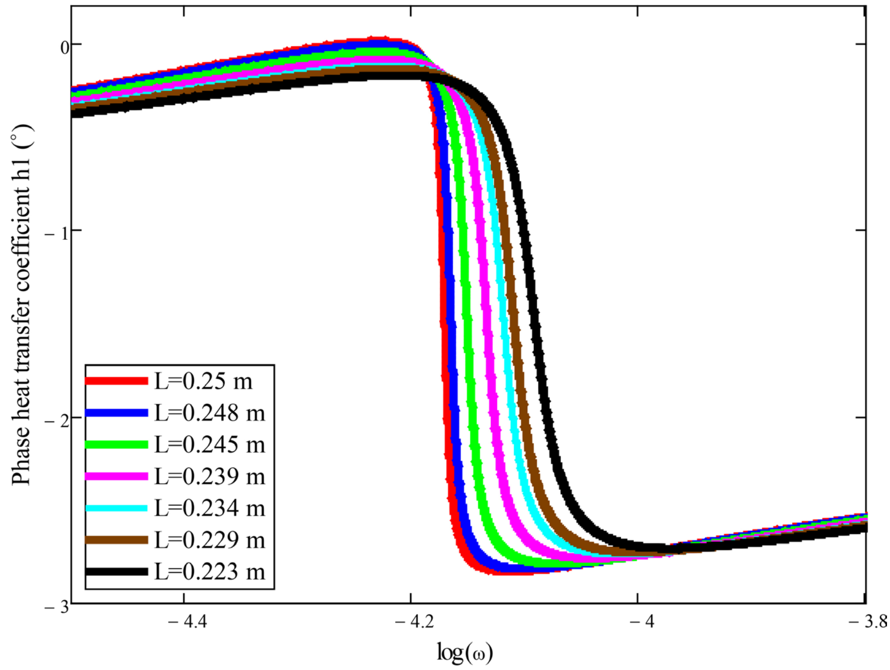

Figure 6. Phase of h_1 as function of excitation pulse; influence of thickness.

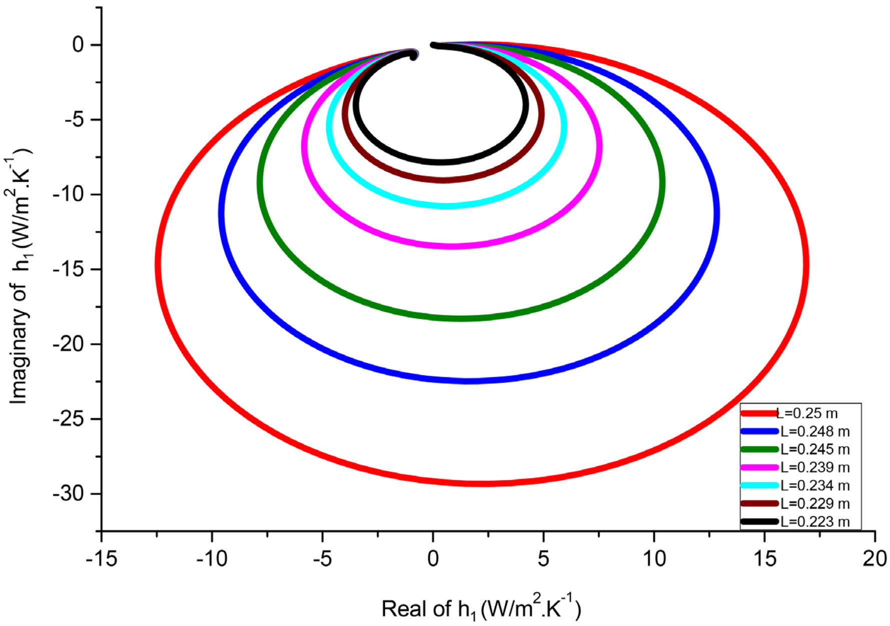

Figure 7. Nyquist representation of h_1; influence of thickness.

These graphs make it possible to highlight equivalent electrical phenomena of typha panel such as capacitive, inductive or resistive aspects [14] [30] [31] [32] [33].

For values of $10^{-4.4} \le \omega \le 10^{-4.2}$, heat transfer coefficient phase changes slightly in an almost linear way. For $\omega \ge 10^{-4.2}$, phase decreases considerably and this decrease is even more important when thickness is significant.

The phase is negative or zero which corresponds to an equivalent electrical circuit in R, L, C where the capacitive phenomena prevail over the inductive phenomena [30] [31] [32] [33].

4. Conclusion

In this article, method of characterizing heat transfer to face of material is studied from heat exchange coefficient. It was then evaluated order of magnitude of this coefficient in relation to optimal insulation thickness of typha panel. Indeed, it has been shown that convection coefficient influences insulation thickness, heat transfer coefficient is an important factor to consider when choosing the insulation thickness.

Conflicts of Interest

The authors declare no conflicts of interest regarding the publication of this paper.

References

[1] Meukam, P., Noumowe, A., Jannot, Y. and Duval, R. (2003) Thermo Physical and Mechanical Characterization of Stabilized Clay Bricks for Building Thermal Insulation. *Materials and Structures*, **36**, 453-460. https://doi.org/10.1007/BF02481525

[2] Shankland, I. (1990) CFC Alternatives for Thermal Insulation Foams. *International Journal of Refrigeration*, **13**, 113-121. https://doi.org/10.1016/0140-7007(90)90010-T

[3] Annabi, M., Mokhtari, A. and Hafrad, T.A. (2006) Estimation Energy Performance of the Building in the Maghreb Context. *Revue des Energies Renouvelables*, **9**, 99-106.

[4] Mounir, S., Khabbazi, A., Khaldoun, A., Maaloufa, Y. and El Hamdounia, Y. (2015) Thermal Inertia and Thermal Properties of the Composite Material Clay-Wool. *Sustainable Cities and Society*, **19**, 191-199. https://doi.org/10.1016/j.scs.2015.07.018

[5] Bouchair, A. (2008) Steady State Theoretical Model of Fired Clay Hollow Bricks for Enhanced External Wall Thermal Insulation. *Building and Environment*, **43**, 1603-1618. https://doi.org/10.1016/j.buildenv.2007.10.005

[6] Chatain, S. and Gonella, C. (1998) Conductive and Radiative Transfers in Building Materials: State the Art and Recent Progress. *La Revue de Métallurgie Paris*, **95**, 1149-1156. https://doi.org/10.1051/metal/199895091149

[7] Brodt, K.H. and Bart, G.C. (1994) Performance of Sealed Evacuated Panels as Thermal Insulation. *International Journal of Refrigeration*, **17**, 257-262. https://doi.org/10.1016/0140-7007(94)90042-6

[8] Kari, B., Perrin, B. and Foures, J.-C. (1992) Macroscopic Modeling of Heat and Humidity Transfers in Building Materials. The Necessary Data. *Materials and Structures*, **25**, 482-489. https://doi.org/10.1007/BF02472638

[9] Nicolas, J., Rivez, J.-F. and Liefrig, J. (1988) Energy Management of Single Family Homes with High Inertia Slabs and Storage in Pebbles. *Revue Générale de Thermique*, **33**, 557-584.

[10] Fabien, S. (2008) Physico-Chemical Pollutants in Indoor Air: Sources and Health Impacts. *Environnement risque et santé*, **7**, 425-430.

[11] Voumbo, M.L., Wereme, A., Gaye, S., Adj, M. and Sissoko, G. (2010) Characterization of the Thermo Physical Properties of Kapok. *Research Journal of Applied Sciences*, *Engineering and Technology*, **2**, 143-148.

[12] Benkaddour, M., Aoual, F.K. and Semcha, A. (2009) Durability of Mortars Based on Natural Pozzolan and Artificial Pozzolan. *Revue Nature et Technologie*, **1**, 63-73.

[13] Voumbo, M.L., Wereme, A. and Sissoko, G. (2010) Characterization of Locals Insulators: Sawdust and Wool of Kapok. *Research Journal of Applied Sciences*, *Engineering and Technology*, **2**, 138-142.

[14] Diouf, A., Diagne, I., Ould Brahim, M.S., Sow, M.L., Niang, F. and Sissoko, G. (2013) Study in Cylindrical Coordinates of the Heat Transfer Through a Tow Material-Thermal-Impedance. *Research Journal of Applied Sciences*, *Engineering and Technology*, **5**, 5159-5163. https://doi.org/10.19026/rjaset.5.4259

[15] Chabi, E., Doko, V., Agoua, E., Olodo, E., Adjovi, E.C. and Merlin, E. (2016) Formulation of Rice Husk Concrete: Study of Shear and Punching-Bending Behavior. *Afrique Science*, **12**, 114-124.

[16] Bah, O.M., Ndiaye, M.B., Traoré, Y., Faye, S., Diagne, I., Gomina, M. and Sissoko, G. (2018) Determination of the Study Frequency Band of a Kenaf Material from the Evaluation of the Temperature and the Heat Flux Density as a Function of the Excitation Frequency. *International Journal of Innovation and Applied Studies*, **24**, 1917-1922.

[17] Khaine, D., Desmons, J.Y., Khaine, A., Ben Younes, R. and Le Ray, M. (1999) Simulation of the Thermal Behavior of a Room by the Method of Green's Functions. *International Journal of Thermal Sciences*, **38**, 340-347. https://doi.org/10.1016/S1290-0729(99)80100-8

[18] Ben Amor, S., Fathallah, R., Boukadida, N. and Guedri, L. (2008) Contribution to the Study of Heat Transfers in a Room with a Structure with Variable Insulation. *Revue des Energies Renouvelables CISM'*08, Oum El Bouaghi, 79-88.

[19] Necib, H., Belakroum, R. and Belakroum, K. (2016) Improvement of Thermal Insulation of Habitats in Hot and Arid Regions. 3*rd International Conference on Energy*, *Materials*, *Applied Energetics and Pollution*, Constantine, 30-31 October 2016, 964-971.

[20] Dahli, M. and Toubal, R. (2010) Thermal Insulating Material Based on Household and Olive Waste. *Revue des Energies Renouvelables*, **13**, 339-346.

[21] Alamdari, F. and Hammond, G.P. (1983) Improved Data Correlations for Buoyancy-Driven Convection in Rooms. *Building Services Engineering Research and Technology*, **4**, 106-112. https://doi.org/10.1177/014362448300400304

[22] Khalifa, A.J.N. and Marshall, R.H. (1990) Validation of Heat Transfer Coefficients on Interior Building Surfaces Using a Real-Sized Indoor Test Cell. *International Journal Heat Mass Transfer*, **33**, 2219-2236. https://doi.org/10.1016/0017-9310(90)90122-B

[23] Jayamaha, S.E.G., Wijeysundera, N.E. and Chou, S.K. (1996) Measurement of the Heat Transfer Coefficient for Wall. *Building and Environment*, **31**, 399-407. https://doi.org/10.1016/0360-1323(96)00014-5

[24] Min, T.C., Schutrum, L.F., Parmelee, V.G. and Vouris, J.D. (1956) Natural Convection and Radiation in a Panel Heated Room. *ASHRAE Transactions*, **62**, 337-358.

[25] Defraeye, T., Blocken, B. and Carmeliet, J. (2011) Convective Heat Transfer Coefficients for Exterior Building Surfaces: Existing Correlations and CFD Modelling. *Energy Conversion and Management*, **52**, 512-522. https://doi.org/10.1016/j.enconman.2010.07.026

[26] McAdams, W.H. (1942) Heat Transmission. McGraw-Hill, Kogakusha.

[27] Diaw, A.S., Sow, D., Ndiaye, M.B., Abdelakh, A.O., Wade, M. and Gaye, S. (2016) Valorization of *Typha australis* by Its Integration in Building Construction Materials. *The International Journal of Emerging Technology and Advanced Engineering*, **6**, 34-37.

[28] Meukam, P., Jannot, Y., Noumowe, A. and Kofane, T.C. (2004) Thermo Physical Characteristics of Economical Building Materials. *International Journal Construction and Building Materials*, **18**, 437-443. https://doi.org/10.1016/j.conbuildmat.2004.03.010

[29] Youssou, T., Ndeye, T., Moustapha, T., Amary, T., Lamine, B.M., *et al.* (2019) AC Recombination Velocity in the Back Surface of a Lamella Silicon Solar Cell under Temperature. *Journal of Modern Physics*, **10**, 1235-1246. https://www.scirp.org/journal/jmp https://doi.org/10.4236/jmp.2019.1010082

[30] Ould Brahim, M.S., Diagne, I., Tamba, S., Niang, F. and Sissoko, G. (2011) Characterization of the Minimum Effective Layer of Thermal Insulation Material Tow-Plaster from the Method of Thermal Impedance. *Research Journal of Applied Science, Engineering and Technology*, **3**, 338-344. http://www.maxwellsci.com

[31] Diouf, A., Diagne, I., Oul Brahim, M.S., Sow, M.L., Niang, F. and Sissoko, G. (2013) Study in Cylindrical Coordinates of the Heat Transfer through a Tow Material-Thermal Impedance. *Research Journal of Applied Sciences, Engineering and Technology*, **5**, 5159-5163. http://www.maxwellsci.com https://doi.org/10.19026/rjaset.5.4259

[32] Ould Cheikh, K., Diagne, I., Sow, M.L., Ould Brahim, M.S., Diouf, A., Diallo, K., Dieng, M. and Sissoko, G. (2013) Interpretation of the Phenomena of Heat Transfer from Representations of Nyquist and Bode Plots. *Research Journal of Applied Sciences, Engineering and Technology*, **5**, 1118-1122. http://www.maxwellsci.com https://doi.org/10.19026/rjaset.5.4824

[33] Diallo, A.K., Boukar, M., Ndiaye, M.A., *et al.* (2014) Study of the Equivalent Electrical Capacity of a Thermal Insulating Kapok-Plaster Material in Frequency Dynamic Regime Established. *Research Journal of Applied Sciences, Engineering and Technology*, **8**, 2141-2145. http://www.maxwellsci.com https://doi.org/10.19026/rjaset.8.1210